Quantum Storage of Heralded Polarization Qubits in Birefringent and Anisotropically Absorbing Materials

Christoph Clausen, Félix Bussières, Mikael Afzelius,* and Nicolas Gisin
Group of Applied Physics, University of Geneva, CH-1211 Geneva 4, Switzerland
(Received 17 January 2012; published 10 May 2012)

Storage of quantum information encoded into heralded single photons is an essential constituent of long-distance quantum communication based on quantum repeaters and of optical quantum information processing. The storage of photonic polarization qubits is, however, difficult because many materials are birefringent and have polarization-dependent absorption. Here we present a simple scheme that eliminates these polarization effects, and we demonstrate it by storing heralded polarization qubits into a solid-state quantum memory. The quantum memory is implemented with a biaxial yttrium orthosilicate (Y_2SiO_5) crystal doped with rare-earth ions. Heralded single photons generated from a filtered spontaneous parametric down-conversion source are stored, and quantum state tomography of the retrieved polarization state reveals an average fidelity of $97.5 \pm 0.4\%$, which is significantly higher than what is achievable with a *measure-and-prepare* strategy.

DOI: 10.1103/PhysRevLett.108.190503 PACS numbers: 03.67.Hk, 42.50.Ex, 42.50.Gy, 42.50.Md

Optical quantum memories [1] allow storage of quantum coherence and entanglement through the reversible mapping of quantum states of light onto matter. They are an essential component of long-distance quantum communication schemes based on quantum repeaters [2] and of distributed quantum networks [3]. A crucial property of quantum memories is the ability to operate with true single photons (i.e., single-photon Fock states) that can encode qubits using various degrees of freedoms, such as temporal modes or polarization. Polarization qubits are widely used, owing to the simplicity in performing arbitrary single-qubit gates and projection measurements. Compatibility of quantum memories with this type of encoding is essential for quantum networks. However, the storage of a qubit in an arbitrary state of polarization is generally difficult because many quantum memories are birefringent and have a polarization-dependent absorption, e.g., solid-state devices. This not only leads to an efficiency that depends on the state to be stored, but also introduces a state dependent polarization transformation. Means to avoid this drawback were investigated with memory-specific approaches [4–9] based on polarization-selection rules of suitably chosen atomic transitions. Another approach, that can in principle work for any type of quantum memory, is based on the embedding of two quantum memories into the arms of an interferometer [10–12], which inevitably requires long-term interferometric stability.

In this Letter, we demonstrate the first storage of heralded polarization qubits into a solid-state quantum memory using a simple and stable scheme compensating for birefringence and absorption anisotropy. The qubits are encoded in heralded single photons generated from spontaneous parametric down-conversion and the quantum memory is realized with birefringent crystals doped with rare-earth ions [13]. In recent years, this type of quantum memory experienced rapid progress and key properties were demonstrated, such as long storage times [14], high-efficiency storage [15] and large temporal multimode capacity [16,17]. Operation at the single-photon level was demonstrated [18] using the atomic frequency comb protocol [19]. This recently led to the conditional detection of time-bin qubits stored in a waveguide [20], the storage of time-bin entangled photons [21,22], and to the heralded creation of entanglement between two crystals [23]. Here, we experimentally show for the first time that these crystals can simultaneously store heralded polarization qubits with high fidelity and maintain their single-photon character. Our scheme can in principle work for all photon-echo-based quantum memories, independent of the material used for the implementation.

Our scheme is illustrated in Fig. 1(a) using two identical quantum memories M_A and M_B of length L each. Both memories are placed along the z-axis such that their input facet is oriented to contain two of the principal axes of the index of refraction, that we label D_1 and D_2, and M_B is rotated at 90° (around z) with respect to M_A. Light propagates along $+z$ and hits the memories at normal incidence. We assume that the principal axes of absorption coincide with D_1 and D_2. We denote α_1 (or α_2) the absorption coefficient along D_1 (or D_2), and $d_1 = \alpha_1 L$ (or $d_2 = \alpha_2 L$) the associated optical depth. The coincidence between the principal axes of index of refraction and absorption is satisfied by many types of quantum memories, such as rare-earth-ion-doped crystals of high symmetry [24]. Hence, the two linear polarizations states parallel to D_1 and D_2 are eigenstates of each memory and form an orthonormal basis that we use to decompose an arbitrary polarization state. Inside M_A, the components will experience different absorption and phase shifts such that an arbitrary polarization input state undergoes a nonunitary

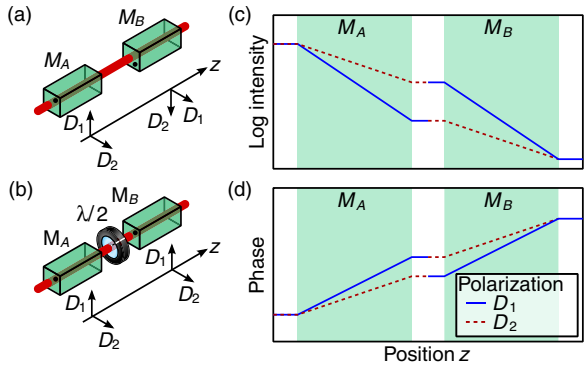

FIG. 1 (color online). Scheme for compensating birefringence and absorption anisotropy using two identical quantum memories M_A and M_B. (a) Light propagates along $+z$. The principal axes of the index of refraction D_1 and D_2 of each memory are orthogonal to z, and M_B is rotated 90° around z with respect to M_A. This arrangement creates a quantum memory that is polarization preserving and has a constant efficiency for all input polarization states. (b) Alternatively, a wave plate can be inserted between M_A and M_B. (c) Light intensity and (d) accumulated optical phase along the two-memory arrangement for light polarized along D_1 or D_2. The total transmission and phase are the same for both components, and hence for any linear combination.

transformation stemming from the combined effect of birefringence and absorption anisotropy [25]. Nevertheless, the two-memory configuration is such that after passing through both M_A and M_B, both components experience the same total absorption and global phase shift, and the arrangement is uniformly absorbing and polarization-preserving. Using a rigorous decomposition of the whole memory into infinitesimal longitudinal elements, we can show that the memory efficiency of the forward reemitted light can be the same for all polarizations, and that the polarization is preserved [26]. The same conclusion holds with the configuration of Fig. 1(b) where, instead of rotating M_B, a half-wave plate inserted between M_A and M_B swaps the eigenstates (here, the output polarization is preserved up to the swap operation).

We note that the high fidelity of our scheme is conditioned on the interferometric stability of the distance between the two memories, but only on the time scale of the storage time. This condition is experimentally simple to satisfy, especially if the two memories are mounted in a spatial configuration yielding common mode rejection of vibration. In particular, this is easier to satisfy than the long-term stability over the ensemble of all measurements that is required for the scheme based on memories embedded in a Mach-Zehnder interferometer [10–12].

We shall now present a series of measurements made with a pair of 1 cm long Nd^{3+}:Y_2SiO_5 crystals for which we explicitly verified that the principal axes of the index of refraction and of absorption coincide. We stress that the host biaxial crystal is highly birefringent, with a polarization beat length on the order of 100 μm at 883 nm [27]. First, we show that the dependence of the optical depth on the polarization of the light can be strongly attenuated. As a consequence, the efficiency of the quantum memory is practically constant. Second, we use the quantum memory for storage and retrieval of heralded single photons with several polarizations, and obtain the fidelity of the storage process using quantum state tomography.

We first measured the total optical depth d on the ${}^4I_{9/2} \rightarrow {}^4F_{3/2}$ transition at 883 nm of the pair of Nd^{3+}:Y_2SiO_5 crystals, cooled down to 3 K, while varying the polarization of the incident light. The optical depth is obtained through $P_{\text{out}} = P_{\text{in}} e^{-d}$, where P_{in} (or P_{out}) is the optical power before (or after) the two crystals. The two crystals were initially in the configuration of Fig. 1(b), but without the wave plate between the crystals. The measured optical depth is shown in Fig. 2(a). Without the compensation scheme, the absorption varies strongly with the linear polarization state, as expected. The overall absorption for any linear polarization can be calculated by decomposing the light into its components along the two principal axes, such that the overall optical depth is given by [28],

$$d = -\ln(e^{-d_1}\cos^2\phi + e^{-d_2}\sin^2\phi), \tag{1}$$

where d_1 (or d_2) is the optical depth for polarization along D_1 (or D_2), and ϕ the angle of the linear polarization with respect to D_1. A fit of the data to Eq. (1) results in values $d_1 = 2.70(1)$ and $d_2 = 0.99(1)$. These values are consistent with previous measurements performed on single crystals [16]. We then repeated the measurement using the compensation scheme of Fig. 1(b). With compensation, the minimum and maximum values of the optical depth, obtained from another fit to Eq. (1), were found to be 1.68 (1) and 1.98(1). We believe the residual variation can be attributed to a slight misalignment of the crystals with respect to each other, and possibly to unequal crystal lengths. Additionally, it is possible that the retardance and orientation of the half-wave plate deviated from the ideal value and that the windows on the cryostat were slightly birefringent. These last two effects could be avoided by using the configuration of Fig. 1(a).

The optical depth is important for the efficiency of the quantum memory. In the case of the atomic frequency comb (AFC) storage protocol, the efficiency varies as $\eta \propto \tilde{d}^2 e^{-\tilde{d}}$, where $\tilde{d} = d/\mathcal{F}$ is the effective optical depth of the comb, including a dependence on the comb finesse $\mathcal{F}$ [19]. This means that variations in the optical depth translate directly to variations in the memory efficiency. We verified this using the same setup as for the measurement of the optical depth, but now the crystals were prepared as 120 MHz wide atomic frequency combs with a preprogrammed storage time of 50 ns (see [21,23] for details). Using laser pulses of roughly Gaussian shape with 18 ns full width at half maximum, we measured the memory

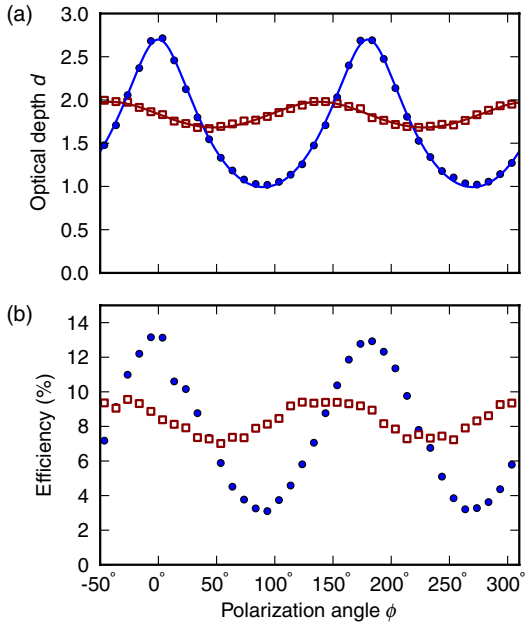

FIG. 2 (color online). Measurements of (a) optical depth and (b) memory efficiency of two Nd^{3+}:Y_2SiO_5 crystals without (●) and with (□) compensation scheme. Incident light is linearly polarized, and the x-axis indicates the angle of the polarization with respect to the D_1 axis of the crystals. (a) Without compensation the optical depth varies between 2.70(1) and 0.99(1), corresponding to propagation along the two optical extinction axes. With compensation the peak-to-peak variation is reduced to 16% of the mean optical depth. Lines are fits to Eq. (1). (b) Efficiency of 50 ns storage measured using laser pulses. With compensation the efficiency is almost independent of polarization.

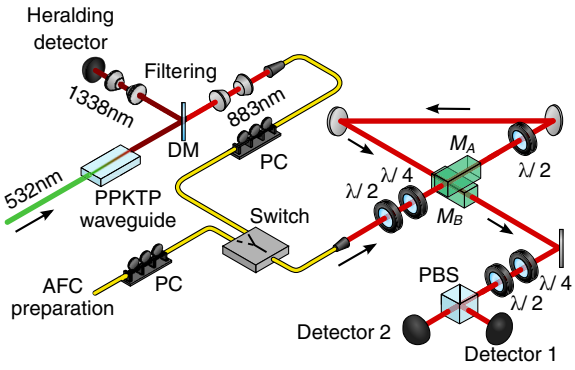

FIG. 3 (color online). Experimental setup for polarization qubit tomography. Pairs of photons are generated by spontaneous parametric down-conversion in a periodically poled KTP waveguide pumped with 4 mW of light from a continuous-wave laser at 532 nm, separated by a dichroic mirror (DM) and strongly filtered. The detection of a photon at 1338 nm on a superconducting nanowire single-photon detector heralds the presence of a single photon at 883 nm. The latter is in resonance with the crystal quantum memories M_A and M_B (where M_A is placed above M_B inside the same cryostat) and acts as a polarization qubit. The initial state of the qubit is prepared using a fiber-based polarization controller (PC) and two wave plates ($\lambda/2$ and $\lambda/4$). A half-wave plate compensates for their anisotropy. Finally, the polarization state of the retrieved photon is analyzed using two more wave plates ($\lambda/4$ and $\lambda/2$) and a polarizing beam splitter (PBS) with a silicon avalanche photo diode at each output. Another polarization controller is used to ensure that the quantum memory is always prepared with the same polarization.

efficiency, that is, the ratio of the area of the retrieved pulse to that of the input pulse, as a function of polarization. Figure 2(b) shows that the efficiency follows the same trend as the optical depth, varying from 3% to 13% without, and from 7% to 9.5% with compensation. We note that the light used for the AFC preparation is more intense in the first crystal. This could mean that the AFCs prepared in both crystals are not identical. Results of Fig. 2(b) show, however, that any difference must be small. This effect could be avoided by pumping the crystals from the sides [15].

Let us now turn to the storage and retrieval of polarization qubits. The complete setup for this purpose is shown in Fig. 3. The experimental cycle consists of two phases of 15 ms each. In the first phase the inhomogeneous absorption of the two crystals is shaped into an atomic frequency comb by optical pumping during 11 ms (see [21] for details). A waiting time of 4 ms is added to avoid fluorescence from atoms left in the excited state. In the second phase the storage, retrieval and analysis of polarization qubits, encoded on heralded single photons, is performed. Our photon source is described in detail elsewhere [21,23]. Photon pairs are generated by spontaneous parametric down-conversion in a periodically poled waveguide. The signal and idler photons with wavelengths 883 and 1338 nm, respectively, are separated and strongly filtered to match the bandwidth of the quantum memories. The detection of an idler photon heralds the presence of a signal photon, which will act as the polarization qubit. The signal photon then passes through a fiber-based polarization controller, a half-wave plate and a quarter-wave plate to prepare the state of the qubit to be stored. Both crystals are placed on top of each other inside one cryostat and are subjected to the same external magnetic field that is necessary to obtain the Zeeman splitting of the ground state of the neodymium ions [16] (this arrangement is compatible with the configuration of Fig. 1(b) only, but this limitation is not fundamental and the configuration Fig. 1(a) would be possible with a slight modification.) The output of the quantum memory is sent towards a polarization analyzer consisting of a quarter-wave plate, a half-wave plate, a polarizing beam splitter and two silicon-based single-photon detectors. Note that the light that prepares the atomic frequency comb passes through the same wave plates as the single photons. A fiber-based polarization controller is used to ensure the preparation light is always linearly polarized along the D_1 axis of M_A.

To show that our compensation method allows for faithful storage of polarization qubits, we performed quantum

TABLE I. Results of the measurements performed on the stored and released single photons for various input states. The fidelity was found via tomographic state-reconstruction using a maximum likelihood method, and the errors estimated via Monte-Carlo simulation. Additionally, the cross-correlation between signal and idler photons $\bar{g}^{(2)}_{si}$, averaged over measurement settings and detectors, indicates the quantum character of the process. The fifth input state is obtained by sending $|H\rangle$ through a quarter-wave plate oriented such that $\alpha = (1 + i\sqrt{2})/2$ and $\beta = 1/2$.

Input State	Fidelity	$\bar{g}^{(2)}_{si}$
$\|H\rangle$	99.3(6)%	7.6(3)
$\|V\rangle$	97(1)%	6.0(3)
$\|L\rangle$	97.7(6)%	9.4(3)
$\frac{1}{\sqrt{2}}(\|H\rangle + \|V\rangle)$	95(1)%	8.0(3)
$\alpha\|H\rangle + \beta\|V\rangle$	98.7(9)%	9.2(3)

state tomography [29] on a set of five different input states. The results are shown in Table I. For each tomographic reconstruction we performed measurements along the three principal axes of the Poincaré sphere, and all detections were conditioned on the simultaneous detection of an idler photon.

Based on the measured number of coincidences, we reconstructed the density matrix of the retrieved qubit by maximum likelihood estimation [29]. The fidelity with respect to the input state is shown in Table I. We also estimated the uncertainty on the fidelity using a Monte-Carlo simulation based on the Poissonian statistics of the detection events. In all cases we find fidelities $F \gtrsim 95\%$, which significantly surpasses the limit of $2/3$ of any classical memory based on a *measure-and-prepare* strategy [30]. This proves that we have implemented a quantum memory that preserves arbitrary states of polarization to a high degree. We attribute the deviation from unit fidelity to imperfections in the state preparation, anisotropy compensation and analysis, caused by nonideal wave plates.

Finally, we investigated the quantum nature of the storage process. First, a measurement of the zero-time autocorrelation function of the heralded signal photon (before storage) yielded $g^{(2)}_{s|i} < 0.06$, which confirms the single-photon nature of the polarization qubit to be stored. The nonclassicality of the photon retrieved from the memory can then be revealed with another measurement, namely, the zero-time intensity cross-correlation $g^{(2)}_{si}$ between signal and idler fields. Specifically, assuming autocorrelations $g^{(2)}_{x}$ for signal and idler fields of $1 \leq g^{(2)}_{x} \leq 2$, where $x = s$ for signal and i for idler, the signature of nonclassicality between both fields becomes $g^{(2)}_{si} > 2$ [31]. We measured values between $\bar{g}^{(2)}_{si} = 6.0(3)$ and $\bar{g}^{(2)}_{si} = 9.4(3)$ for all the stored polarization states, confirming the quantum nature of the storage and retrieval process. The lowest cross-correlation value allows to upper bound the autocorrelation of the retrieved signal photon to $g^{(2)}_{s|i} \leq 0.61(3)$, which is still below the classical threshold of 1 (the upper bound is obtained by assuming that the source is exactly described by a two-mode squeezed state [23]). We note that the relatively large increase of $g^{(2)}_{s|i}$ before and after storage is almost entirely due to an experimental artifact associated with the continuous wave operation of our source of photon pairs [23], and not to a detrimental effect stemming from the memory itself.

To conclude, we have experimentally demonstrated a scheme that allows the faithful storage of polarization qubits encoded into true single photons using a material that is birefringent and has anisotropic absorption. We note that the efficiency of a photon-echo based quantum memory with reemission in the forward mode is limited to 54% [19,32]. To overcome this limitation, and possibly reach 100% efficiency, one possibility is to use the impedance-matched quantum memory scheme in which a forward-emitting quantum memory is placed between two-mirrors with reflectivity chosen such that all the incident light can be absorbed and reemitted [33,34]. Our scheme thus has the potential for demonstrating a high-efficiency solid-state quantum memory that is compatible with polarization qubits. It is particularly well-suited for rare-earth-ions-doped crystals and greatly extends their range of application. For example, the storage of both polarization and temporal modes leads to new interesting possibilities, such as the quantum storage of hyperentangled photons [35].

We thank Imam Usmani, Nicolas Sangouard, and Philippe Goldner for stimulating discussions. We acknowledge support by the Swiss NCCR Quantum Photonics, the Science and Technology Cooperation Program Switzerland-Russia, as well as by the European projects QuRep and ERC-Qore. F. B. was supported in part by le Fond Québécois de la Recherche sur la Nature et les Technologies.

Related results were obtained by other groups in parallel to this work [36,37].

*mikael.afzelius@unige.ch

[1] A. I. Lvovsky, B. C. Sanders, and W. Tittel, Nature Photon. **3**, 706 (2009).
[2] N. Sangouard, C. Simon, H. de Riedmatten, and N. Gisin, Rev. Mod. Phys. **83**, 33 (2011).
[3] H. J. Kimble, Nature (London) **453**, 1023 (2008).
[4] D. N. Matsukevich, T. Chaneliere, S. D. Jenkins, S.-Y. Lan, T. A. B. Kennedy, and A. Kuzmich, Phys. Rev. Lett. **96**, 030405 (2006).
[5] F. Carreño and M. A. Antón, Opt. Commun. **283**, 4787 (2010).
[6] H. P. Specht, C. Nolleke, A. Reiserer, M. Upho, E. Figueroa, S. Ritter, and G. Rempe, Nature (London) **473**, 190 (2011).

[7] M. Lettner, M. Mücke, S. Riedl, C. Vo, C. Hahn, S. Baur, J. Bochmann, S. Ritter, S. Dürr, and G. Rempe, Phys. Rev. Lett. **106**, 210503 (2011).
[8] D. Viscor, A. Ferraro, Y. Loiko, R. Corbalán, J. Mompart, and V. Ahunger, J. Phys. B **44**, 195504 (2011).
[9] S. Riedl, M. Lettner, C. Vo, S. Baur, G. Rempe, and S. Dürr, Phys. Rev. A **85**, 022318 (2012).
[10] Y.-W. Cho and Y.-H. Kim, Opt. Express **18**, 25786 (2010).
[11] H. Zhang, X.-M. Jin, J. Yang, H.-N. Dai, S.-J. Yang, T.- M. Zhao, J. Rui, Y. He, X. Jiang, F. Yang, G.-S. Pan, Z.-S. Yuan, Y. Deng, Z.-B. Chen, X.-H. Bao, S. Chen, B. Zhao, and J.-W. Pan, Nature Photon. **5**, 628 (2011).
[12] D. G. England, P. S. Michelberger, T. F. M. Champion, K. F. Reim, K. C. Lee, M. R. Sprague, X.-M. Jin, N. K. Langford, W. S. Kolthammer, J. Nunn, and I. A. Walmsley, arXiv:1112.0900.
[13] W. Tittel, M. Afzelius, T. Chaneliere, R. Cone, S. Kroll, S. Moiseev, and M. Sellars, Laser Photon. Rev. **4**, 244 (2010).
[14] J. J. Longdell, E. Fraval, M. J. Sellars, and N. B. Manson, Phys. Rev. Lett. **95**, 063601 (2005).
[15] M. P. Hedges, J. J. Longdell, Y. Li, and M. J. Sellars, Nature (London) **465**, 1052 (2010).
[16] I. Usmani, M. Afzelius, H. de Riedmatten, and N. Gisin, Nature Commun. **1**, 12 (2010).
[17] M. Bonarota, J.-L. L. Gouët, and T. Chaneliere, New J. Phys. **13**, 013013 (2011).
[18] H. de Riedmatten, M. Afzelius, M. U. Staudt, C. Simon, and N. Gisin, Nature (London) **456**, 773 (2008).
[19] M. Afzelius, C. Simon, H. de Riedmatten, and N. Gisin, Phys. Rev. A **79**, 052329 (2009).
[20] E. Saglamyurek, N. Sinclair, J. Jin, J. A. Slater, D. Oblak, F. Bussières, M. George, R. Ricken, W. Sohler, and W. Tittel, Phys. Rev. Lett. **108**, 083602 (2012).
[21] C. Clausen, I. Usmani, F. Bussières, N. Sangouard, M. Afzelius, H. de Riedmatten, and N. Gisin, Nature (London) **469**, 508 (2011).
[22] E. Saglamyurek, N. Sinclair, J. Jin, J. A. Slater, D. Oblak, F. Bussières, M. George, R. Ricken, W. Sohler, and W. Tittel, Nature (London) **469**, 512 (2011).
[23] I. Usmani, C. Clausen, F. Bussières, N. Sangouard, M. Afzelius, and N. Gisin, Nature Photon. **6**, 234 (2012).
[24] M. Born and E. Wolf, *Principles of Optics* (Pergamon Press, Oxford, 1965).
[25] B. Huttner, C. Geiser, and N. Gisin, IEEE J. Sel. Top. Quantum Electron. **6**, 317 (2000).
[26] See Supplemental Material at http://link.aps.org/supplemental/10.1103/PhysRevLett.108.190503 for a detailed theoretical treatment of the compensation scheme.
[27] R. Beach, M. Shinn, L. Davis, R. Solarz, and W. Krupke, IEEE J. Quantum Electron. **26**, 1405 (1990).
[28] M. Afzelius, M. U. Staudt, H. de Riedmatten, N. Gisin, O. Guillot-Noël, P. Goldner, R. Marino, P. Porcher, E. Cavalli, and M. Bettinelli, J. Lumin. **130**, 1566 (2010).
[29] J. B. Altepeter, E. R. Jerey, and P. G. Kwiat, *Advances in Atomic, Molecular and Optical Physics* (Elsevier, New York, 2006) Chap. 3.
[30] S. Massar and S. Popescu, Phys. Rev. Lett. **74**, 1259 (1995).
[31] A. Kuzmich, W. P. Bowen, A. D. Boozer, A. Boca, C. W. Chou, L.-M. Duan, and H. J. Kimble, Nature (London) **423**, 731 (2003).
[32] N. Sangouard, C. Simon, M. Afzelius, and N. Gisin, Phys. Rev. A **75**, 032327 (2007).
[33] M. Afzelius and C. Simon, Phys. Rev. A **82**, 022310 (2010).
[34] S. A. Moiseev, S. N. Andrianov, and F. F. Gubaidullin, Phys. Rev. A **82**, 022311 (2010).
[35] J. T. Barreiro, N. K. Langford, N. A. Peters, and P. G. Kwiat, Phys. Rev. Lett. **95**, 260501 (2005).
[36] M. Gündoğan, P. M. Ledingham, A. Almasi, M. Cristiani, and H. de Riedmatten, following paper, Phys. Rev. Lett. **108**, 190504 (2012).
[37] Z.-Q. Zhou, W.-B. Lin, M. Yang, C.-F. Li, and G.-C. Guo, this issue, Phys. Rev. Lett. **108**, 190505 (2012).